Generation of femtosecond extreme ultraviolet pulses using low-energy electron beams for a pump-probe experiment

Ji-Gwang Hwang[a,*], Eun-San Kim[b,*]

[a]Helmholtz-Zentrum Berlin (HZB), Albert-Einstein-straβe 15, 12489 Berlin, Germany
[b]Department of Accelerator Science, Korea University Sejeong Campus, Sejong 339-700, South Korea

Abstract

The surface recombination process and molecular dynamics are generally on the order of tens of femtoseconds; therefore, the research and development of an accelerator-based intense and short-pulse generation scheme are needed for pump-probe experiments, which are widely utilized tools for investigating fast molecular dynamics. Here, we propose an echo-enabled harmonic generation (EEHG)-technique-based free electron laser (FEL) scheme that uses a low-energy beam ($KE \sim 200$ MeV). The proposed scheme is designed to generate short-pulse soft extreme ultraviolet radiation at ~ 80 nm, with a pulse duration of 3 fs for the full width at half maximum. An electron injector consisting of a photo-cathode-based S-band radio frequency electron-gun, solenoid magnets, and three S-band accelerating columns was designed and optimized using a multiobjective particle swarm optimization method. For the EEHG-FEL section, the narrow bands of electrons produced by a second modulator and a few-cycle laser pulse with a linear momentum compaction at the second chicane had a perfect upright position at the top of the current modulation produced by the first modulator, which enhanced the peak current by a factor of approximately 30 %. In this scheme, two conventional lasers with wavelengths of 5.2 µm and 800 nm were adopted to enhance the high bunching factors by generating microbunching structures. The saturated output power of the proposed FEL was approximately 4.97 MW.

Keywords: Femtosecond extreme ultraviolet (EUV) pulse generation, Short-pulse generation, Echo-enable harmonic generation (EEHG), Low-energy electron beam injector

1. Introduction

To utilize pump-probe experiments, there is strong scientific motivation to generate strong, ultra-short, and temporally coherent extreme ultraviolet (EUV) radiation to investigate numerous areas of fast molecular dynamics in a multidisciplinary field because the surface recombination process and molecular dynamics in materials are generally on the order of tens of femtoseconds. In particular, EUV is a promising tool for investigating biological materials. During the past decade, many free electron laser (FEL) facilities [1–6] such as FLASH and the European XFEL in Germany, LCLS in the USA, SACLA in Japan, PAL-XFEL in Korea, and SwissFEL in Switzerland have started operations based on the self-amplified spontaneous emission (SASE) principle [7, 8], which has been technologically proven and can produce excellent transverse coherent light. However, the SASE-FEL has limited temporal coherence. Many FELs based on seeding techniques for generating strong and short EUV and X-ray pulses using high-energy electron beams have been and are being launched [9–12] to obtain intense and highly temporal coherent light. An echo-enabled harmonic generation (EEHG) technique [13–15] with proven performance for generating nearly Fourier-transform limited pulses with better stabilities for the central wavelength and intensity [9] makes it possible

*Corresponding authors
Email addresses: ji-gwang.hwang@helmholtz-berlin.de (Ji-Gwang Hwang), eskim1@korea.ac.kr (Eun-San Kim)

to produce short pulses in the sub-femtosecond range [16]. Recently, the design and construction of in-vacuum undulators with period lengths of a few centimeters have been carried out in many laboratories to obtain higher-energy photons with lower harmonics for the undulator radiation [17–21]. The combination of these two frontier technologies extends to the generation of a soft EUV pulse at the fundamental mode of an undulator using a low-energy electron beam. Here, we propose a production method for a femtosecond-short soft-EUV pulse with a wavelength of ~ 80 nm using an electron beam of approximately 200 MeV. This technique also shows the possibility of adjusting the time delay between the short pulse from the electron radiation and the laser pulse with high precision.

In the first part of this paper, we describe the physical design and optimization of an electron injector consisting of a 1.6-cell S-band radio-frequency (RF) gun, three S-band accelerating columns, six quadrupole magnets, and two solenoids to produce a high-quality electron beam. Since the performance of EEHG-FEL depends strongly on electron beam parameters, the design and optimization of the low energy electron beam injector were performed to obtain reliable calculation results of the EEHG-FEL. The basic idea of this method for short-pulse generation is presented in the second part, along with a numerical example to illustrate it. In this example, we demonstrate the feasibility of generating a 3 fs full width at half maximum (FWHM) EUV pulse tuned to the wavelength of 80 nm.

2. Electron beam injector design and optimization

An accelerator can be categorized as an electron beam injector for generating high-quality and short electron beams, and as an EEHG-FEL for producing high harmonics in the electron beam density distribution for the generation of short-wavelength radiation. The schematic layout of our scheme is shown in Fig. 1.

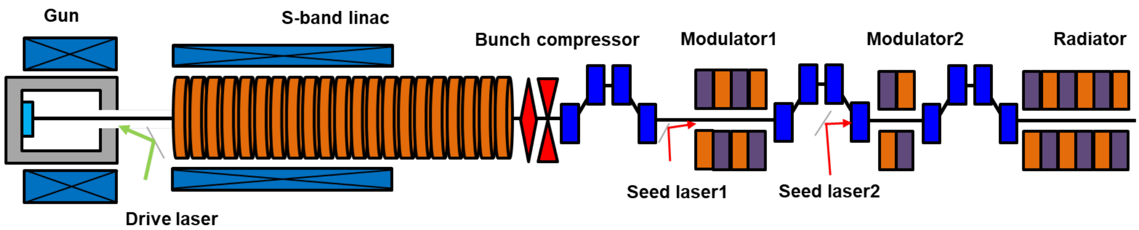

Figure 1: Schematic of femtosecond pulse generation using low-energy electron beams. The accelerator consists of an electron injector with 1.6-cell S-band photocathode RF gun, solenoid magnets, three S-band accelerating columns, a bunch compressor, and an EEHG-FEL with two modulators, two chicanes, two seeding lasers, and a radiator.

The performance of the photo-injector, which consisted of a 1.6-cell photo-cathode-based RF electron-gun, solenoid magnets, and S-band accelerating columns, was proven by generating low-emittance beams in a 6-D phase-space with a high peak current [22]. In our macro-particle tracking simulation, the S-band RF gun was adopted to produce low-emittance beams, and two solenoid magnets were placed at the gun and first meter of the first accelerating column to compensate for the emittance growth by a space-charge force. Three accelerating column sections based on a three-meter Stanford Linear Accelerator Center (SLAC) traveling wave structure were used after the gun accelerated the beam to 228 MeV. Quadrupole doublets were installed between the accelerating columns to adjust the betatron functions at the entrance of the FEL section.

In order to achieve small transverse emittances, as well as a short bunch length for a high peak current, all parameters, including the phase and voltage of the gun and cavities, and strengths of the solenoid and quadrupole magnets, were optimized using a multiobjective particle swarm optimization (MOPSO) method, which is an interesting nature-inspired algorithm that mimics the social cooperative and competitive behavior of bird flocking and fish schooling [23, 24]. The MOPSO python module is compatible with the particle tracking simulation using the 3D algorithm of the ASTRA [25]. The ASTRA tracks macroparticles through user-defined external fields, including the space-charge field of the particle distribution. The initial distribution used in the simulation used the virtual cathode drive laser image as a transverse profile. The

MOPSO-based optimization can run on parallel processors, making 3D calculations time efficient. The optimization results are shown in Fig. 2.

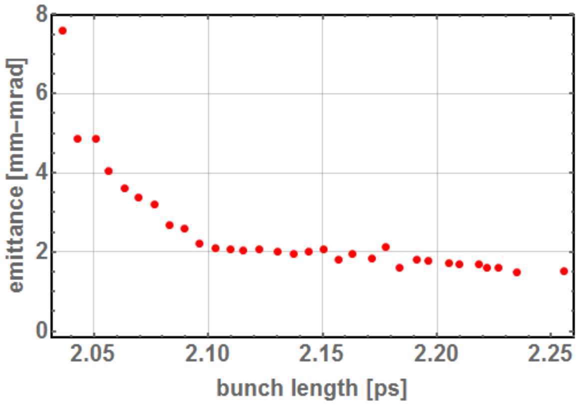

Figure 2: Optimization results using multiobjective particle swarm optimization (MOPSO) method with ASTRA code. The transverse emittance is a function of the bunch length. The transverse emittances strongly rely on the bunch length as a result of the space-charge force.

Because of the space-charge force, the transverse emittances are inversely proportional to the bunch length. The design employs a gun with an optical spot size at the cathode with a radius of 1.2 mm and a pulse duration with a uniform pulse of 10 ps and 0.7 ps rise time. It corresponds to a thermal emittance of 0.3 mm-mrad. The initial coordinates of the 200k macro particles were used for the tracking simulation. The evolution of the transverse emittances and energy for the optimum value is shown in Fig. 3.

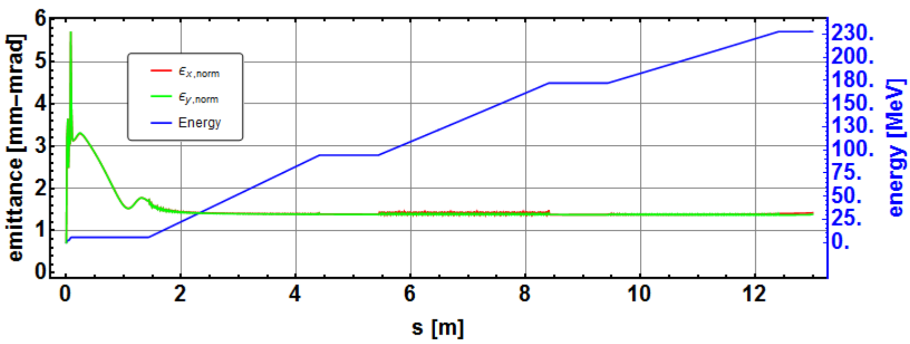

Figure 3: Evolution of normalized transverse emittances and energy at 1 nC along electron injector for settings optimized by MOPSO method. All parameters were calculated by a tracking simulation with 200k macroparticles.

The peak electric field in the gun was 121 MV/m at the cathode, and the laser was injected at 20° ahead of an on-crest phase. This introduced an energy spread of approximately 1.8 % rms for the full beam at the exit of the gun but slightly helped in the emittance compensation. This energy spread was removed in the first accelerating section by phasing the RF such that the beam arrived slightly behind the crest. In the first accelerating column, the centroid of the beam was 6.82° behind the crest, and the average axial electric field was 30.5 MV/m. The average axial electric fields of the second and third accelerating sections were 28.2 MV/m and 20.1 MV/m, respectively. The optimum strength of the solenoid magnet placed at the electron gun for emittance compensation was 2.76 kG. The phase-space particle distributions are shown in Fig. 4.

The phase ellipse angle mismatching of a few slices of the bunch was observed in the horizontal phase-space. This caused the growth of a projected emittance. The injector provided electron beams with a bunch charge of 1 nC, a bunch length of 2.32 ps rms, normalized horizontal and vertical emittances of 1.42 mm-

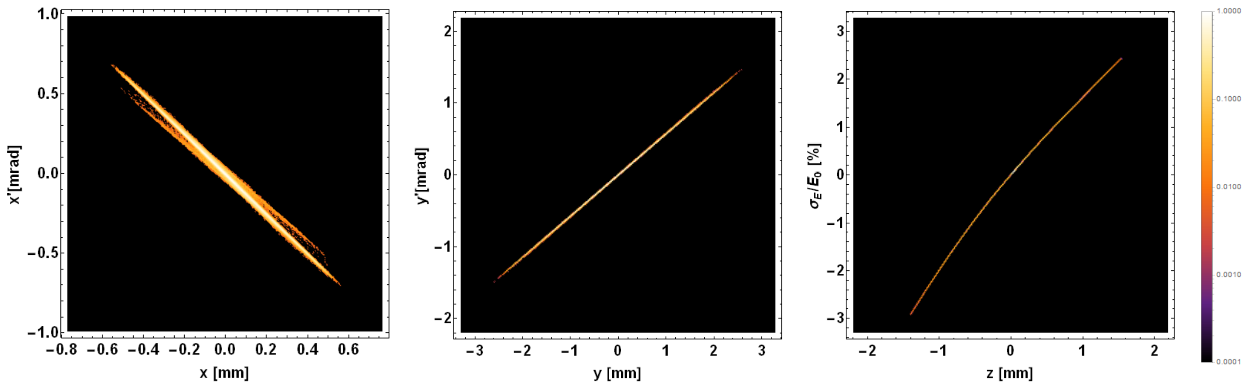

Figure 4: ASTRA output of phase-space distribution of electron beam at end of electron injector with energy of 228 MeV, transverse normalized emittances of 1.4 mm-mrad rms, and energy spread of 1.2 % rms. The energy chirp made it possible to compress the bunch length in the bunch compressor installed upstream of the EEHG-FEL section.

mrad rms, and an energy spread of 1.2 % rms at a kinetic energy of 228 MeV. The electron beam parameters are listed in Table 1.

Table 1: Electron beam parameters at end of injector. The peak current could be enhanced by the bunch compressor installed upstream of the EEHG-FEL section.

Parameter	Unit	Value
Beam energy	MeV	228
Bunch charge	nC	1
Peak current	kA	0.14
Energy spread, rms	%	1.2
Bunch length, rms	ps	2.32
Normalized emittances, rms	mm-mrad	1.42

In general, the performance of a FEL can be determined by the various slices and the relevant interplay with the evolution of the associated transverse phase-space distributions [26]. The performance of the short-pulse EEHG-FEL scheme, however, was mainly determined by the slice emittances and peak current because the method utilized a few tens of femtoseconds of the whole bunch. The slice emittance and peak current at the end of the electron injector were calculated and are shown in Fig. 5.

The horizontal and vertical slice emittances at the center of the bunch were approximately 1 mm-mrad, and the peak current was 0.14 kA. The energy chirp in the longitudinal phase-space, which was a correlation between the longitudinal positions and energies of the particles, made it possible to compress the bunch length in the bunch compressor installed upstream of the EEHG-FEL section. The electron bunch could be compressed by a factor of 10–20, which made it possible to achieve a peak current of 1–2 kA. More details about theoretical and experimental studies for the bunch compressor design with low energy beams are in Ref. [26–30]. In addition, we can adjust bunch charges from nC to pC to avoid an emittance degradation effect.

3. EEHG-FEL design

An EEHG-FEL is a laser-assisted electron beam manipulation scheme designed to produce high harmonics in the beam density distribution for the generation of short-wavelength radiation. The key advantage of the EEHG technique is that it can generate very high harmonics with a harmonic number much larger than the ratio of the energy modulation to energy spread [31]. In this regime, the beam can then serve as a high-quality seed in a downstream FEL for the emission of fully coherent light at short wavelengths. To numerically illustrate the feasibility of a short and intense pulse generation scheme using the EEHG-FEL technique, we demonstrated the generation of a few femtosecond EUV pulses with a carrier frequency of 80

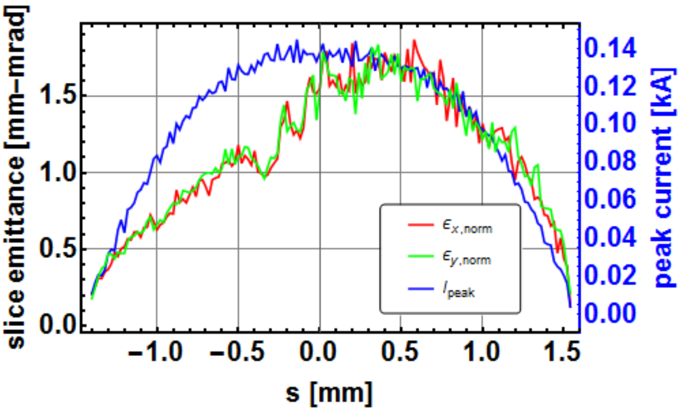

Figure 5: Simulated slice emittances and peak current at end of injector beam line.

nm using two laser pulses and two modulators for the energy modulation, two chicanes for manipulating the energy modulation to density modulation, and one radiator. The design values were carefully optimized to enhance the microbunching structure inside the spikes of the peak current because it was given by combining the values of the two chicanes and laser power. For a small modulation amplitude with high linear momentum compaction, R_{56}, microbunching with a small period corresponding to a harmonic number was effective, in accordance with Ref. [32]. However, the current modulation by the first stage, in this case, completely vanished as a result of the high linear momentum compaction factor at the first chicane.

Here, we propose a method by which the narrow bands of electrons produced by a second modulator and a few-cycle laser pulse with linear momentum compaction at the second chicane take a perfectly upright position at the top of the current modulation produced by the first modulator, which makes it possible to enhance the peak current by a factor of approximately 30 %. Because the radiation power for a coherent process was proportional to the square of the number of electrons in a slice, it could enhance the radiation power by a factor of 70 %. The current can be optimized by selecting a small R_{56} as much as small energy modulation in the first modulator. The parameters were selected to maximize the microbunching inside the central spike of the peak current, as well as the current modulation at the first stage. It was calculated numerically. For the calculation of the 1D distribution, it was assumed that the cross-section of the laser light in the modulator was several times larger than the transverse beam sizes of the bunch in all of the modulators where a seed laser interacted with a bunch. Therefore, all electrons at the same location in the bunch received equal energy gains according to the phase of the laser light. In particular, the energy modulation of the bunch was independent of jitter in the relative timing of the bunch and laser because the laser pulse was longer than the bunch for the first modulator. The detailed parameters of the modulators, magnetic chicanes, and lasers are listed in Table 2.

Table 2: Electron beam parameters.

Parameter	Unit	Value
$R_{56}^{(1)}$	mm	0.52
Laser1 power	mJ	1.54
Laser1 wavelength (λ_1)	µm	5.2
Modulator1 period length	cm	5
Modulator1 period		33
$R_{56}^{(2)}$	µm	12
Laser2 power	µJ	466
Laser2 wavelength (λ_2)	nm	800
Modulator2 period length	cm	5
Modulator2 period		12

The electron bunch interacted with a long laser pulse having a wavelength of 5.2 µm inside the first modulator containing approximately 33 periods. A laser power of 1.54 mJ, which is commercially available, was required to generate the energy modulation of 4 σ_E in the first modulator. The modulator had a period length of 5 cm, and the wiggler parameter was chosen to satisfy the FEL resonance condition. A few-cycle laser pulse with carrier-envelope phase stabilization [33], a carrier wavelength of 800 nm, and a pulse length of 3.5 fs FWHM was used for the selective energy modulation of the electrons within a few femtosecond long section of the electron bunch in the second modulator. The laser power was 466 µJ, and the second modulator had 12 periods with a period length of 5 cm. Based on the parameters, the longitudinal phase-space distribution of the electrons at the entrance of the radiator is shown in Fig. 6.

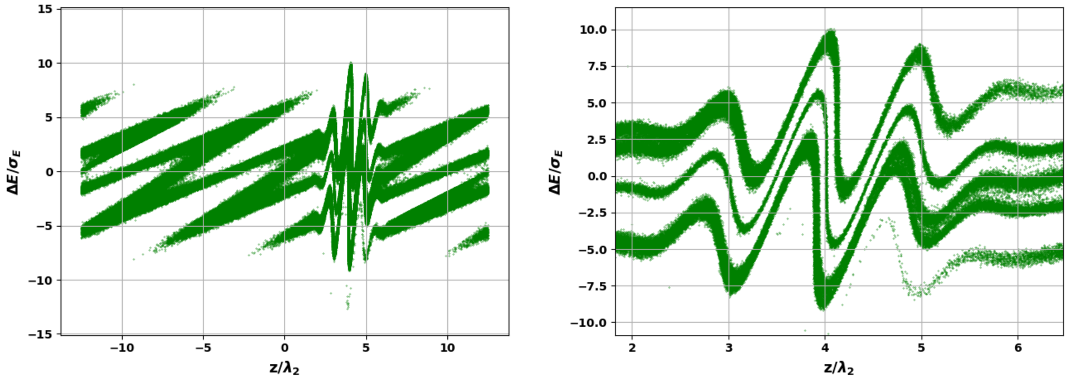

Figure 6: Longitudinal phase-space distribution of electrons at entrance of radiator (left) and a fragment of the longitudinal phase-space showing the microstructure inside the central peak (right). It was calculated under the assumption that the cross-section of the laser light in the modulator was several times larger than the transverse beam sizes of the bunch in all modulators.

The phase for the electric field with respect to the envelope was adjusted so that there was a zero field at the center of the laser pulse. Because the R_{56} value of the first chicane was not large enough to remove the density modulation, the density modulation was observed in the current profile. Thus, the center of the second laser pulse was synchronized with the high current. After the second modulator, the electron bunch passed the second dispersive magnetic chicane, whose strength (12 µm) was much smaller than the R_{56} value of the first dispersive magnetic chicane. As a result, we obtained the pattern of current enhancement, which was large at the central peak and smaller at the two side peaks (Fig. 7).

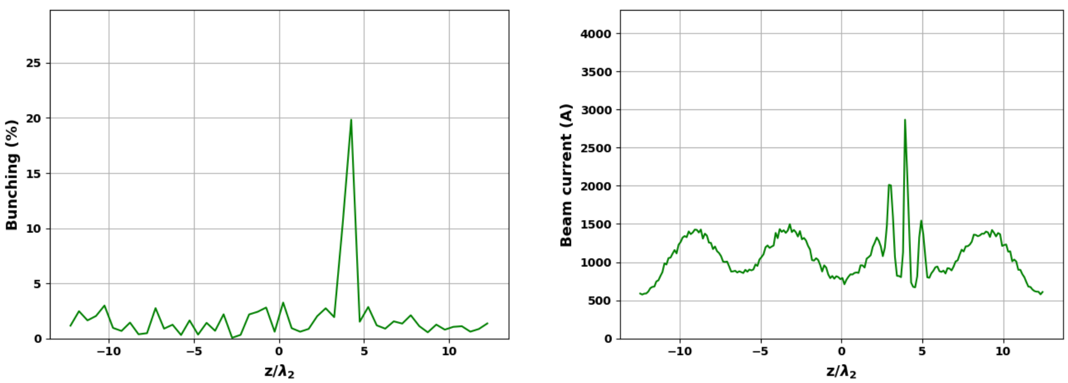

Figure 7: Bunching factor and peak current of the beam. The enhancement in the peak current due to the longitudinal phase-space manipulation by the energy modulation in the interaction with the laser pulse and density variation by the R_{56} in the chicane.

Further downstream is the radiator with 16 periods, a period length of 16 mm, and dimensionless undulator parameter $K = 1.03$ tuned for the FEL resonance at a wavelength of 80 nm. Fig. 8 shows the calculations carried out using GENESIS [34] with an initial particle distribution prepared with the 1D code, where the bunched electrons produced a dominant pulse of coherent EUV radiation, including transverse coherence, with 3.0 fs FWHM (see Fig. 9).

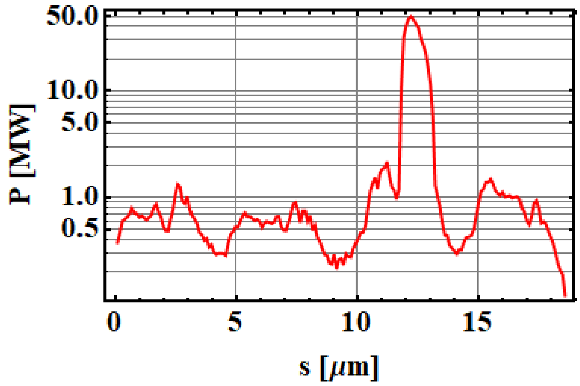

Figure 8: Radiation output at radiator on logarithmic scale. It was calculated using GENESIS with an initial particle distribution prepared with the 1D code. The bunched electrons produce a dominant pulse of coherent EUV radiation, at approximately 80 nm, including transverse coherence, with 3.0 fs FWHM.

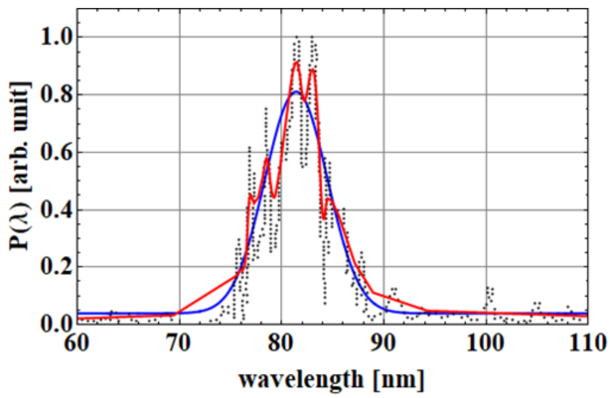

Figure 9: Spectrum of short EUV pulse produced by electron bunch radiating in radiator. Total power of the radiation is 4.97 MW, and the spectral width is 3.06 nm rms.

4. Discussion

The coherent radiation of the short EEHG pulse will be superimposed on the incoherent radiation of the rest of the beam. The rest of the beam, however, produces incoherent radiation with a broad spectrum since the radiator has only 16 periods with period length of 16 mm. Thus we can enhance the contrast ratio by tuning a monochromator which is widely used to select a wavelength of the radiation.

In addition to the short-pulse generation scheme, we also have a plan to operate a single-stage EEHG at high harmonics to directly generate an intense EUV radiation pulse and SASE-FEL at a fundamental frequency for generating a terahertz radiation pulse because the modulator and radiator cover all of the frequency ranges. In the single-stage EEHG, long seed laser pulses can be adopted to fully cover the electron bunch, which results in a much higher output pulse energy and much narrower output bandwidth.

5. Summary

The physical design and optimization of an electron injector, which consisted of a 1.6-cell S-band photocathode RF gun, two solenoids for emittance compensation, three S-band traveling wave structures, and quadrupole magnets, for generating high-quality electron beams were performed. The optimization of the parameters was performed using MOPSO method, which was compatible with the particle tracking simulation using the 3D algorithm of the ASTRA. The injector provided electron beams with a bunch charge of 1 nC, a bunch length of 2.32 ps rms, normalized horizontal and vertical emittances of 1.42 mm-mrad rms, and an energy spread of 1.2 % rms at a kinetic energy of 228 MeV. At the end of the injector, a bunch compressor was installed to compress the bunch length because the radiation power for a coherent process was proportional to the square of the number of electrons in a slice. It made it possible to enhance the peak current up to a few kiloamps. In addition, we also proposed a method wherein the narrow bands of electrons produced by a second modulator and a few-cycle laser pulse with linear momentum compaction at the second chicane took a perfectly upright position at the top of the current modulation produced by the first modulator, which made it possible to enhance the peak current by a factor of approximately 30 %. With the proposed FEL design, we demonstrated the possibility of generating a short and intense EUV pulse in the radiator with 16 periods, a period length of 16 mm, and dimensionless undulator parameter $K = 1.03$ tuned for the FEL resonance at a wavelength of 80 nm. The numerical calculation was carried out using GENESIS with the initial particle distribution prepared with a 1D code. The bunched electrons produced a dominant pulse of coherent EUV radiation, including transverse coherence, with 3.0 fs FWHM. The total power was 4.97 MW.

6. Acknowledgement

The authors wish to thank their colleagues in Helmholtz-Zentrum Berlin (HZB), Ji Li and M. Ruprecht, for providing the python module for multiobjective particle swarm optimization (MOPSO) that they developed. This work has been supported by German Bundesministerium für Bildung und Forschung, Land Berlin, and grants of Helmholtz Association.

[1] W. A. Ackermann, et al. Nat. Photonics, 1, 336 (2007).
[2] P. Emma, et al. Nat. Photonics, 4, 641 (2010).
[3] T. Ishikawa, et al. Nat. Photonics, 6, 540 (2012).
[4] J. H. Han, H. S. Kang, I. S. Ko, Status of the PAL-XFEL project. In Proceedings of the IPAC2012, New Orleans, LA, USA, 20–25 May 2012; 1735–1737.
[5] R. Ganter, SwissFEL-Conceptual Design Report, No. PSI-10-04; Paul Scherrer Institute (PSI): Villigen, Switzerland, 2010.
[6] A. Massimo, The European X-ray Free-Electron laser: Technical Design Report; European XFEL Project Team, Hamburg, Germany, 2013.
[7] A. M. Kondratenko and E. L. Saldin, Part. Accel., 10, 207 (1980).
[8] R. Bonifacio, C. Pellegrini, and L. M. Narducci, Opt. Commun., 50, 373 (1984).
[9] Z. Zhao, et al., Appl. Sci., 7, 607 (2017).
[10] E. Allaria, et al., Nat. Photonics, 7, 913 (2013).
[11] B. Liu, et al. Phys. Rev. Spec. Top. Accel. Beams, 16, 020704 (2013)
[12] E. Hemsing, et al. Nat. Photonics, 10, 512 (2016)
[13] G. Stupakov, Phys. Rev. Lett., 102, 074801 (2009).
[14] D. Xiang and G. Stupakov Phys. Rev. STAB, 12, 256 (2009).
[15] D. Xiang and G. Stupakov Phys. Rev. STAB, 17, 070702 (2014).
[16] A. Zholents and G. Penn, Nucl. Instr. Methods A, 612, 254 (2010).
[17] S. Yamamoto, et al., J. Appl. Phys., 74, 500 (1993).
[18] J. Chavanne et al., Synchrotron Rad. News, 28, 3, 15 (2015).
[19] S. H. Kim et al., IEEE Transactions on Applied Superconductivity, 15, 2, 1240 (2005).
[20] J. Bahrdt et al., Proc. of FEL Conference, Trieste, Italy, 610-613 (2004).
[21] A. Temnykh, Phys. Rev. ST Accel. Beams, 11, 120702, (2008).
[22] D. H. Dowell, et al., Proc. of EPAC 2004, Lucerne, Switzerland, 500 (2004).
[23] P. K. Tripathi and S. Bandyopadhyay, S. K. Pal, Information Sciences, 177, 5033 (2007).
[24] J. Li, et al., Proc. of IPAC2017, Copenhagen, Denmark, THPAB008 (2017).
[25] K. Floettmann, "ASTRA User Manual", www.desy.de/ mpyflo/Astra documentation.
[26] G. Dattoli, et al. Nucl. Instr. Methods A, 671, 51 (2012).
[27] U. Lehnert, et al., Proc. of IPAC 2014, Dresden, Germany, TUPRO044 (2014).
[28] B. R. P. Gamage and T. Satogata, Proc. of PAC 2013, Pasadena, USA, THPHO21 (2013).

[29] M. Abo-Bakr, B. Kuske and A. Matveenko, Proc. of IPAC'10, Kyoto, Japan, TUPD102 (2010).
[30] M. Shimada and R. Hajima, Phys. Rev. ST Accel. Beams, 13, 1007701 (2010).
[31] E. Hemsing, et al. Phys. Rev. ST Accel. Beams, 17, 070702 (2014).
[32] A.Zholents, Phys. Rev. ST Accel. Beams, 8, 040701 (2005).
[33] F. Krausz and M.Ivanov, Rev. Mod. Phys., 81, 163 (2009).
[34] S. Reiche, Nucl. Instr. Methods A, 429, 243 (1999).